MINERALOGICAL MAGAZINE, DECEMBER 1995, VOL. 59, PP 750–754

High-Ti biotite bearing ignimbrites from the Zilan Valley near Ercis, Lake Van, Eastern Turkey

COLLISION-RELATED Neogene volcanism in Eastern Turkey is thought to have begun in the Late Miocene (Innocenti *et al.*, 1976, 1980; Pearce *et al.*, 1990). In the Zilan Valley, north of Ercis, calcalkaline intermediate–acid volcanic rocks (Arslan, 1994) include ignimbrites containing high-Ti biotite. The ignimbrites were first described by Innocenti *et al.* (1980) who gave K–Ar ages of 4.6–5.9 ± 0.2 Ma. The Aquitanian-Late Burdigalian limestone, sandstone and marl underlying the volcanic rocks do not contain any volcanic material. So volcanic activity in the area started after the Late Burdigalian (Innocenti *et al.*, 1980) in the Serravalian as confirmed by K–Ar dating of 13.1 Ma (Innocenti *et al.*, 1976). Three volcanic cycles followed: early calcalkaline, alkaline and late calcalkaline rocks, and the ignimbrites occur in the early calcalkaline cycle.

Ignimbrite flows are best exposed west of Evbeyli village, Semikayalari Sirti, northwest of Kuzubulak Golu, southeast of Isbasi village and Demek Tepe, and are 0–75 m in thickness. There were three main phases, the lowest black, glassy and horizontally fractured, the next being cream-coloured and tuffaceous, with sedimentary structures (parallel lamination, graded bedding and cross bedding) and the upper being less glassy. Among these ignimbrite flows, unwelded tuffs are present which show lateral transition to the ignimbrites.

Petrography

The ignimbrites vary in texture, mineralogy, degree of welding and compaction from trachytic to rhyolitic types. Generally, they contain a mixture of rock fragments, crystals, glass shards and glassy pumice fragments. Eutaxitic fabrics with intense welding, compaction and alignment of flattened glassy pumice fragments and elongated curved glass shards are very characteristic. The vitroclastic fraction ranges from abundant to zero.

The average crystal size is a few mm and may be finer towards the top of the unit. The erupted crystals include abundant fresh plagioclase (20–30 %), alkali feldspar (5–7%) and biotite. In addition, resorbed augite, a little olivine, opaque minerals, quartz, amphibole, accessory apatite and zircon are present in lesser amounts (Table 1). All phenocryst phases are commonly fragmented. Quartz crystals are sparse and isolated.

A few anorthoclase phenocrysts show granophyric texture with intergrown quartz. Plagioclase phenocrysts are normally-zoned, sometimes with super-

TABLE 1. Descriptive petrographic features of the ignimbrites

Rock types	Phenocrysts	Groundmass	Fabrics developed
Rhyolite ignimbrite	Quartz Anorthoclase Sanidine (sparse) Plagioclase Biotite Augite	Microcrystalline quartz and feldspar minor biotite, ilmenite, magnetite, accessory apatite, zircon	Devitrified glass shards, pumice fragments, compaction foliation and aggregates of plagioclase and augite
Trachyte ignimbrite	Anorthoclase Sanidine Plagioclase Quartz (sparse)		

imposed low-amplitude oscillatory zoning, and contain inclusions of biotite, apatite and glass. Glass inclusions within them are $An_4Ab_{62}Or_{34}$. Some plagioclase phenocrysts have suffered two periods of partial resorption, producing mottled, high-An zones. This interpretation contrasts with that of Chappell (1978) that these features are characteristic of restite feldspar.

Biotites are large (2–3 mm), euhedral to subhedral red-brown plates, and some are slightly chloritized. They contain opaque oxide, apatite, zircon and plagioclase inclusions. Augite forms subhedral microphenocrysts in glomeroporhyritic clots which suggest accumulation of this phase during differentiation.

The vitroclastic fraction comprises glass shards, flattened or curved and rarely chloritized pumice fragments commonly moulded around crystals. The glassy matrix has an apparently discontinuous or continuous lamination caused by compaction and welding of original pumice fragments. The glassy matrix may show devitrification and recrystallization.

TABLE 2. Chemical analyses of minerals in ignimbrites

Sample	MA- 63 Felds. core	MA-63 Felds. core	MA-74 Feds. core	MA-74 Felds. rim	MA-74 Felds. mic	MA-63 Cpx core	MA-63 Cpx rim	MA-63 Biotite pheno	MA-74 Biotite micro	MA-74 Biotite pheno	MA-229 Pheno Mag.	MA-74 Micro Ilm.
SiO_2	66.50	57.18	63.95	61.96	62.12	50.91	50.37	36.41	37.79	36.99	0.43	0.18
TiO_2	0.15	0.09	0.15	0.10	0.07	0.77	0.99	6.42	5.98	6.61	10.61	38.38
Al_2O_3	18.40	26.06	21.35	23.51	23.19	2.20	2.53	13.29	12.97	13.18	0.66	0.25
FeO*	1.13	0.52	0.37	0.38	0.09	9.10	9.68				85.97	57.31
Fe_2O_3								2.21	2.26	2.32		
FeO								11.25	11.55	11.81		
MnO	0.00	0.00	0.11	0.03	0.00	0.27	0.31	0.38	0.46	0.34	1.61	2.27
MgO	0.15	0.15	0.10	0.02	0.10	16.06	15.71	15.43	16.18	15.70	0.29	0.71
CaO	0.13	7.89	2.57	5.03	4.62	18.38	18.01	0.13	0.00	0.03	0.04	0.00
Na_2O	8.74	6.57	7.54	8.06	8.05	0.54	0.69	1.09	0.81	1.20	0.00	0.03
K_2O	3.90	0.63	3.41	1.27	1.37	0.05	0.00	8.35	8.82	8.81	0.02	0.02
P_2O_5	0.00	0.00	0.02	0.01	0.01	0.00	0.00	0.07	0.00	0.06	0.00	0.00
Cr_2O_3	0.00	0.02	0.00	0.02	0.05	0.20	0.09	0.00	0.00	0.00	0.00	0.05
NiO	0.05	0.00	0.00	0.00	0.00	0.00	0.00	0.05	0.00	0.00	0.00	0.00
Total	99.15	99.11	99.57	100.39	99.67	98.48	98.38	95.08	96.82	97.05	99.63	99.20
Formula on the basis of 32 oxygens for feldspar and magnetite, 6 oxygens for pyroxene and ilmenite, and 22 oxygens for biotite												
Si	11.96	10.37	11.45	11.00	11.05	1.91	1.89	5.42	5.52	5.41	0.01	0.01
Ti	0.02	0.01	0.02	0.01	0.01	0.02	0.03	0.72	0.66	0.72	0.28	0.72
Al	3.90	5.57	4.51	4.92	4.87	0.09	0.11	2.33	2.33	2.27	0.03	0.01
Fe^{2+}	0.17	0.08	0.06	0.06	0.06	0.08	0.10	0.25	0.25	0.25	1.39	0.55
Fe^{3+}						0.20	0.20	1.39	1.41	1.44	1.18	0.64
Mn	0.00	0.00	0.01	0.00	0.00	0.01	0.01	0.05	0.05	0.04	0.05	0.05
Mg	0.00	0.04	0.03	0.01	0.03	0.89	0.88	3.42	3.52	3.42	0.06	0.03
Ca	0.02	1.53	0.49	0.96	0.88	0.74	0.72	0.02	0.00	0.00	0.00	0.00
Na	3.05	2.31	2.62	2.78	2.78	0.04	0.05	0.31	0.23	0.34	0.02	0.00
K	0.89	0.14	0.78	0.29	0.31	0.00	0.00	1.58	1.64	1.64	0.00	0.00
P	0.00	0.00	0.00	0.00	0.00	0.00	0.00	0.01	0.00	0.01	0.00	0.00
Cr	0.00	0.00	0.00	0.00	0.00	0.01	0.00	0.00	0.00	0.00	0.00	0.00
Ni	0.01	0.00	0.00	0.00	0.00	0.00	0.00	0.00	0.00	0.00	0.00	0.00
Total	20.04	20.06	19.97	20.04	20.02	4.00	4.00	15.51	15.52	15.56	3.00	2.00
Mg#						0.76	0.74	0.67	0.68	0.67		
Mn/Mg											3.15	1.83
An	0.60	38.44	12.67	23.79	22.18	Wo 38.27	37.79	Phl. 56.24	58.65	57.07		
Ab	76.83	57.92	67.27	69.05	69.97	En 46.49	45.85	An. 23.01	23.49	24.08		
Or	22.56	3.63	20.05	7.16	7.85	Fs 15.23	16.36					

FeO* is total iron as FeO. Fe^{3+} is calculated by normalization for pyroxene, magnetite and ilmenite, and by ratio for biotite according to Schumacher (1991). Mg# = $Mg/(Mg + Fe^{3+} + Fe^{2+})$.

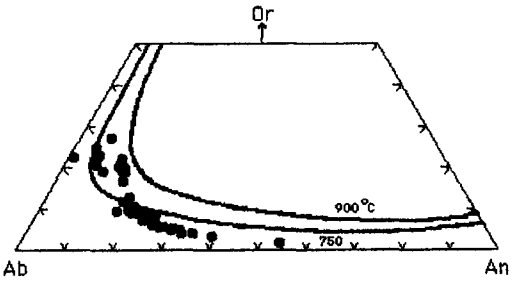

FIG. 1. Ternary feldspar plot. Solvi for coexisting feldpars in equilibria is shown for 750°C at 1 kbar and 900°C at 0.5 kbar (Fuhrman and Lindsley, 1988).

Ignimbrites generally vary in their crystal contents. This reflects the degree of crystallization before eruption, and for crystal-rich types it probably implies significant crystallization in a high-level crustal chamber prior to eruption. Microgranitoid clasts have a similar composition to the average ignimbrite. Thus it may be concluded that the magma reached high levels in a largely liquid state but was preceded by earlier magma which crystallized. Quartz and clinopyroxene appear to have crystallized first, followed by plagioclase, then biotite, and lastly K-feldspar at lower pressure.

Lithic clasts. Lithic clasts up to 1.5 cm are common, and include basalts, rhyolites, microgranitoids and metasedimentary rocks. The volcanic rock fragments include plagioclase ± sanidine, clinopyroxene, abundant opaque oxides, quartz and a glassy matrix. Some of them display porphyritic and microlitic textures, and have calcic plagioclase (An_{53}) and chromian augite ($Wo_{37}En_{48}Fs_{15}$ with Cr_2O_3 = 0.25 wt.%). Microgranitoids include both equigrannlar albite (Ab_{91-93}) with quartz and granophyric K-feldspar and quartz, the latter are typical of high-level granite intrusions. Metasedimentary fragments, interpreted as regional metamorphic rocks, contain quartz, biotite, muscovite, chlorite and clay minerals.

Feldspar. The feldspar varies from oligoclase to anorthoclase (Table 2 and Fig. 1). All the plagioclase, whether phenocrysts, microphenocrysts or microlites, is $An_{20-38}Ab_{58-70}Or_{4-8}$. Some of the larger crystals are normally-zoned An_{38} to An_{18}; some are antiperthitic and some show transition to anorthoclase. Inclusions of unzoned corroded plagioclase in clinopyroxene are labradorite (An_{53}). Anorthoclase phenocrysts are unzoned and average $An_{13}Ab_{67}Or_{20}$ while microlites are $An_6Ab_{67}Or_{27}$.

Clinopyroxene. The pyroxenes are augite (Morimoto *et al.*, 1988) ranging from $Wo_{37}En_{48}Fs_{15}$ to $Wo_{44}En_{40}Fs_{16}$ (Table 2) with low Ti and relatively high Al (0.04 and 0.11 respectively, in the formula unit) which is significant for subalkaline rock types (Le Bas, 1962). The presence of low Ti in the augites contrasts with the biotites which have extremely high Ti contents. This may be due to early crystallization of augites and the presence of the most calcic plagioclase (An_{53}) inclusions within augite phenocrysts supports this interpretation.

Ti-rich biotite. Biotites (Table 2) are extremely Ti-rich phlogopite-annite with $Mg/(Mg+F^{3+}+Fe^{2+})$ 0.66 to 0.70 and TiO_2 ranging from 5.48 to 6.75 wt.%. Phenocrysts have higher Ti than microphenocrysts, suggesting decline of Ti in biotite as crystallization proceeded.

The mechanism of Ti substitution in biotite has been investigated by many authors (Guidotti *et al.*, 1977; Dymek, 1983; Labotka, 1983; Abrecht and Hewitt, 1988; Brigatti *et al.*, 1991) but there is no agreement as to the usual position of Ti in Ti-rich biotites or the mechanism of its substitution. No clear relationship between Al and Ti is shown by Fig. 2, which implies that Ti-Tschermak's substitution was not important. As Ti increases, Mg declines and Fe^{2+} and (Na+K) increase. Generally, substitution of larger Fe^{2+} ions for Mg compensates for the misfit resulting from the substitution of smaller Ti^{4+} ions in octahedral sheets of biotite (Dallmeyer, 1974; Guidotti *et al.*, 1977; Shau *et al.*, 1991). Like many volcanic biotites (De Pieri *et al.*, 1978) Si and Al are insufficient to fill all the tetrahedral sites. Both Ti and Ca generally increase in biotite with increasing temperature (Shau *et al.*, 1991), showing the present biotites to have had a high temperature of crystallization.

Fe-Ti oxides. The two main oxide minerals are ilmenite and, to a lesser extent, magnetite, and both are homogeneous. Magnetites are Ti-rich (TiO_2 10–25 wt%). They contain total FeO between 60 and 74 wt.%, Al_2O_3 from 0.8 to 2 wt.%, MnO 1.33 wt.% to 2.17 wt.%, MgO 0.82 wt.% to 1.24 wt.% but Ni and Cr are very low or absent. Magnetite inclusions within other mineral phases e.g. biotite) have relatively low TiO_2 (~ 5 wt.%). Ilmenites are almost stoichiometric, with respect to $FeTiO_3$, with MgO 0.69 to 2.09 wt.%, minor Cr, V and Al, and MnO between 1.96 and 2.66 wt.%. The distribution of Mg and Mn between the magnetite and the ilmenite indicates equilibrium between these coexisting phases (Bacon and Hirschmann, 1988).

Geothermometry and geobarometry. Ignimbrite feldspars are plotted on a ternary isotherm plot (Fig. 1) based on synthetic ternary feldspar compositions and the thermodynamic data of Fuhrman and Lindsley (1988). On the plot, alkali feldspars, mainly anorthoclase, fall in the temperature field between 750 and 900°C. However, plagioclases in disequilibrium with anorthoclase indicate a temperature below 750°C. Following Anderson and Lindsley (1985), co-existing magnetite and ilmenite phenocrysts give temperatures between 846 and 921°C, and

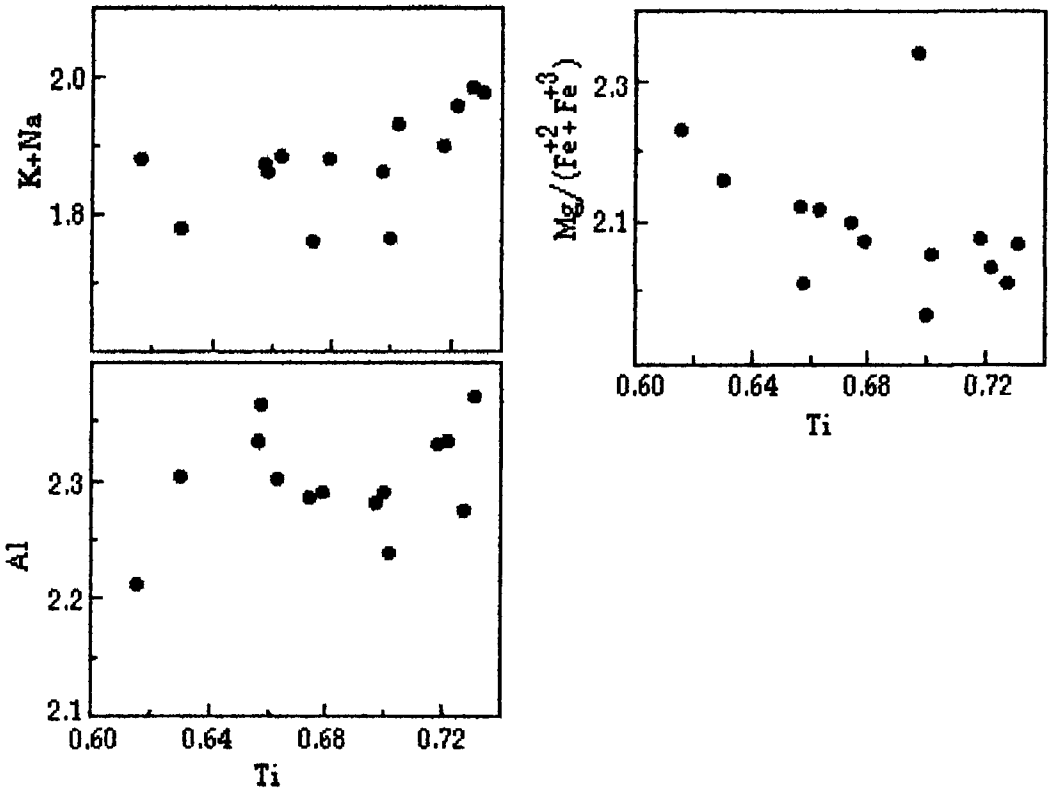

FIG. 2. Biotite chemical variation. Element values are per formula unit.

f_{O_2} between 1.42 and 2.29 relative to the QFM buffer. In the metamorphic enclaves, the presence of muscovite + quartz assemblage indicates a maximum pressure of about 6.5 kbar and a maximum temperature of 725°C (Chatterjee and Johannes, 1974).

Conclusions

Ignimbrites show moderate to strong welding indicating high temperature emplacement. They contain volcanic, granitoid and metamorphic rock fragments. The rocks contain Ti-rich (5.5–6.7 wt.% TiO_2) biotites of high temperature crystallization. Magnetite and ilmenite indicate temperatures of 846–921°C, and f_{O_2} = 1.42–2.29 relative to FMQ. Alkali feldspar and sodic plagioclase in equilibrium indicate 750–900°C. Metamorphic rock assemblages reveal a maximum of 6.5 kbar and 725°C.

Acknowledgements

This research was undertaken as a part of Ph.D. study by M. Arslan at Glasgow University, with the financial support of the Turkish Ministry of Education. We thank the Turkish Ministry of Education for funding the research, the academic and technical staff, especially R. McDonald for his technical assistance on the Cambridge Microscan V microprobe equipped with EDS.

References

Abrecht, J. and Hewitt, D.A. (1988) Experimental evidence on the substitution of Ti in biotite. *Amer. Mineral.*, *73*, 1275–84.

Anderson, D.J. and Lindsley, D.H. New (and final?) models for the Ti-rich magnetite/ilmenite geothermometer and oxygen barometer. *Trans. Amer. Geophys. Un. (EOS)*, **66**, 416.

Arslan, M. (1994) *Mineralogy, geochemistry, petrology and petrogenesis of the Meydan-Zilan (Ercis-Van, Turkey) area volcanic rocks*. Ph.D. thesis, Glasgow University, 559 pp.

Bacon, C.R. and Hirschmann, M.M. (1988) Mg/Mn partitioning as a test for equilibrium between coexisting Fe-Ti oxides. *Amer. Mineral.*, *73*, 57–61.

Brigatti, M.F., Galli, E. and Poppi, L. (1991) Effect of Ti

substitution in biotite-1M crystal chemistry. *Amer. Mineral.*, *76*, 1174–83.

Chappell, B.W. (1978) Granitoids of the Moonbi district, New England Batholith, eastern Australia. *J. Geol. Soc. Austral.*, **25**, 267–84.

Chatterjee, N.D. and Johannes, W. (1974) Thermal stability and standard thermodynamic properties of synthetic $2M_1$-Muscovite, $KAl_2[AlSi_3O_8(OH)_2]$. *Contrib. Mineral. Petrol.*, **48**, 89–114.

De Pieri, R., Gregnanin, A. and Piccirillo, E.M. (1978) Trachyte and rhyolite biotites in the Euganean Hills (NE Italy). *Neues Jahrb. Mineral., Abh.*, **132**, 309–28.

Dymek, R.F. (1983) Titanium, aluminium and interlayer cation distributions in biotite from high-grade gneisses, West Greenland. *Amer. Mineral.*, *68*, 880–99.

Fuhrman, M.L. and Lindsley, D.H. (1988) Ternary-feldspar modelling and thermometry. *Amer. Mineral.*, *73*, 201–15.

Guidotti, C.V., Cheney, J.T. and Guggenhein, S. (1977) Distribution of titanium between coexisting muscovite and biotite in pelitic schists from northwestern Maine *Amer. Mineral.*, *62*, 438–48.

Innocenti, F., Mazzuoli, C., Pasquare, G., Serri, G. and Villari, L. (1980) Geology of the volcanic area North of Lake Van, Turkey. *Geol. Runds.*, **69**, 292–322.

Innocenti, F., Mazzuoli, R., Pasquare, G., Radicati di Brozola, F. and Villari, L. (1976) Evolution of the volcanism in the area of interaction between the Arabian, Anatolian and Iranian plates (Lake Van, Eastern Turkey). *J. Volcanol. Geotherm. Res.*, **1**, 103–12.

Labotka, T.C. (1983) Analyses of the compositional variations of biotite in pelitic hornfelses from northeastern Minnesota. *Amer. Mineral.*, *68*, 900–14.

Le Bas, M.J. (1962) The role of aluminium in igneous clinopyroxenes with relation to their parentage. *Amer. J. Sci.*, *260*, 267–88.

Morimoto, M. (1988) Nomenclature of pyroxenes. *Mineral. Mag.*, **52**, 535–50.

Pearce, J.A., Bender, J.F., De Long, S.E., Kidd, W.S.F., Low, P.J., Guner, Y., Saroglu, F., Yilmaz, Y., Moorbath, S. and Mitchell, J.G. (1990) Genesis of collision volcanism in Eastern Anatolia, Turkey. *J. Geol. Soc.*, **141**, 447–52.

Schumacher, J.C. (1991) Empirical ferric iron correction: necessity, assumptions, and effects on selected geothermobarometers. *Mineral. Mag.*, **55**, 3–18.

Shau, Y.-H., Yang, H.-Y. and Peacor, D.R. (1991) On oriented titanite and rutile inclusions in sagenitic biotite. *Amer. Mineral.*, *76*, 1205–17.

[*Manuscript received 24 February 1995: revised 23 March 1995*]

KEYWORDS: ignimbrite, high-Ti biotite, lithic clasts, ternary isotherm plot.

Department of Geology and Applied Geloogy,
Glasgow University,
Glasgow G12 8QQ,
UK

M. ARSLAN
B.E. LEAKE

MINERALOGICAL MAGAZINE, DECEMBER 1995, VOL. 59, PP 754–757

Tamarugite, $NaAl(SO_4)_2 \cdot 6H_2O$, from Te Kopia, New Zealand

TAMARUGITE, $NaAl(SO_4)_2 \cdot 6H_2O$, is one of a suite of secondary, water soluble, hydrated sulphates reported forming by oxidation of sulphides under dry, usually arid conditions (Palache *et al.*, 1951) although it has also been found near the sea at two localities with moderately high rainfall (Hutton, 1970; Segnit, 1976). In the Te Kopia geothermal area of New Zealand's North Island, where the average annual rainfall is 1165 mm and the climate temperate, the mineral occurs as part of an efflorescence currently forming on hot water altered ignimbrites now undergoing alteration by steam.

The Te Kopia geothermal area is large and vigorously active. It is located in the Taupo Volcanic Zone at latitude 38° 24' S, longitude 176° 13' E and lies astride the west-facing scarp of the upthrown eastern block of the active Paeroa Fault. Altered and steaming ground extends for over 2.5 km along the fault scarp and within 500 m of it Several areas of perched, shallow, steam-heated, acid-